Magnetic-Field Dependences of Thermodynamic Quantities in the Vortex State of Type-II Superconductors

Koichi Watanabe and Takafumi Kita
Division of Physics, Hokkaido University, Sapporo 060-0810, Japan

Masao Arai
National Institute for Materials Science, Namiki 1-1, Tsukuba, Ibaraki 305-0044, Japan

(Dated: February 2, 2008)

We develop an alternative method to solve the Eilenberger equations numerically for the vortex-lattice states of type-II superconductors. Using it, we clarify the magnetic-field and impurity-concentration dependences of the magnetization, the entropy, the Pauli paramagnetism, and the mixing of higher Landau levels in the pair potential for two-dimensional s- and $d_{x^2-y^2}$-wave superconductors with the cylindrical Fermi surface.

PACS numbers: 74.25.Op, 71.18.+y

I. INTRODUCTION

Recent experiments[1,2,3,4,5] have shown that magnetic-field dependences of thermodynamic quantities in the vortex state of type-II superconductors provide unique information on the pairing symmetry and gap anisotropy. On the theoretical side, however, calculations of those quantities still remain a fairly difficult task to perform. The quasiclassical equations derived by Eilenberger[6] provide a convenient starting point for this purpose. Pesch[7] obtained a compact analytic solution to them based on the lowest Landau-level approximation for the pair potential. It has been used recently to discuss the field dependences of the thermal conductivity,[8] the density of states,[9,10,11] and thermodynamic quantities.[12] On the other hand, Klein[13,14] obtained a full numerical solution for the vortex-lattice state using a standard procedure to solve ordinary differential equations. This numerical approach has been used extensively by Ichioka *et al.*[15,16,17,18,19,20,21,22,23] to clarify the field dependences of the pair potential and the density of states for type-II superconductors with various energy-gap structures. It should be noted, however, that those numerical studies all adopted simplified model Fermi surfaces instead of complicated Fermi surfaces for real materials. Indeed, recent theoretical studies[10,24,25,26] have clarified that detailed Fermi-surface structures are indispensable for the quantitative description of the vortex state.

With these backgrounds, we here develop an alternative method to solve the Eilenberger equations for the vortex-lattice states. A key point lies in expanding the pair potential and the quasiclassical f function in the basis functions of the vortex-lattice states, thereby transforming the differential equations into algebraic equations. This method has been powerful for (i) solving the Ginzburg-Landau equations[27] and the Bogoliubov-de Gennes equations[28,29,30,31] and (ii) obtaining quantitative agreements on the upper critical field H_{c2} of Nb, $NbSe_2$, and MgB_2 with Fermi surfaces from first-principles electronic-structure calculations.[25,26] Thus, the method may be more advantageous for the calculations of thermodynamic quantities in finite magnetic fields when realistic Fermi surfaces are used as inputs. It will also be convenient for microscopically calculating responses of the vortex-lattice state to external perturbations,[32] such as vortex-lattice oscillations.

This method is applied here to calculate magnetic-field dependences of the magnetization, the entropy, the Pauli paramagnetism, and the pair potential at various temperatures for the two-dimensional s- and $d_{x^2-y^2}$-wave superconductors in the clean and dirty limits. These quantities have been obtained near H_{c2} for the s-wave pairing.[33,34] Our purpose here is to clarify the overall field dependence of those quantities.

This paper is organized as follows. Section II gives the formulation. Section III presents numerical results. Section IV summarizes the paper. We use $k_{\rm B}=1$ throughout.

II. FORMULATION

A. Eilenberger equations

We take the external magnetic field $\mathbf{H}$ along the z axis and express the vector potential as[6,27,35,36,37,38]

$$\mathbf{A}(\mathbf{r}) = Bx\hat{\mathbf{y}} + \tilde{\mathbf{A}}(\mathbf{r})\,. \tag{1}$$

Here B is the average flux density produced jointly by the external current and the internal supercurrent, and $\tilde{\mathbf{A}}$ is the spatially varying part of the magnetic field satisfying $\int \boldsymbol{\nabla}\times\tilde{\mathbf{A}}\,d\mathbf{r}=\mathbf{0}$. We choose the gauge such that $\boldsymbol{\nabla}\cdot\tilde{\mathbf{A}}=0$.

The Eilenberger equation for the even-parity pairing without Pauli paramagnetism is given by[6,25]

$$\left(\varepsilon_n + \frac{\hbar}{2\tau}\langle g\rangle + \frac{1}{2}\hbar\mathbf{v}_{\rm F}\cdot\boldsymbol{\partial}\right) f = \left(\Delta\phi + \frac{\hbar}{2\tau}\langle f\rangle\right) g\,. \tag{2a}$$

Here $\varepsilon_n=(2n+1)\pi T$ $(n=0,\pm1,\pm2,\cdots)$ is the Matsubara energy with T the temperature, τ is the relaxation time

by nonmagnetic impurity scattering, and $\langle\cdots\rangle$ denotes the Fermi-surface average:

$$\langle g\rangle \equiv \int dS_{\rm F}\frac{g(\varepsilon_n,\mathbf{k}_{\rm F},\mathbf{r})}{(2\pi)^3 N(0)|\mathbf{v}_{\rm F}|}\,,$$

with $dS_{\rm F}$ an infinitesimal area on the Fermi surface, $N(0)$ the density of states per spin and per unit volume at the Fermi energy in the normal state, and $\mathbf{v}_{\rm F}$ the Fermi velocity. The operator $\boldsymbol{\partial}$ in Eq. (2a) is defined by

$$\boldsymbol{\partial} \equiv \boldsymbol{\nabla} - i\frac{2\pi}{\Phi_0}\mathbf{A}\,,$$

with $\Phi_0 \equiv hc/2e$ the flux quantum,[39] $\Delta(\mathbf{r})$ is the pair potential, and $\phi(\mathbf{k}_{\rm F})$ specifies the gap anisotropy satisfying $\langle\phi(\mathbf{k}_{\rm F})\rangle = 1$. Finally, the quasiclassical Green's functions f and g for $\varepsilon_n > 0$ are connected by $g = (1-ff^\dagger)^{1/2}$ with $f^\dagger(\varepsilon_n,\mathbf{k}_{\rm F},\mathbf{r}) = f^*(\varepsilon_n,-\mathbf{k}_{\rm F},\mathbf{r})$.

Equation (2a) has to be solved simultaneously with the self-consistency equation for the pair potential and the Maxwell equation for $\tilde{\mathbf{A}}$, which are given respectively by

$$\Delta(\mathbf{r})\ln\frac{T_{c0}}{T} = 2\pi T\sum_{n=0}^{\infty}\left[\frac{\Delta(\mathbf{r})}{\varepsilon_n} - \langle\phi(\mathbf{k}_{\rm F})f(\varepsilon_n,\mathbf{k}_{\rm F},\mathbf{r})\rangle\right], \tag{2b}$$

$$-\nabla^2\tilde{\mathbf{A}}(\mathbf{r}) = -i\frac{16\pi^2 eN(0)T}{c}\sum_{n=0}^{\infty}\langle\mathbf{v}_{\rm F}g(\varepsilon_n,\mathbf{k}_{\rm F},\mathbf{r})\rangle\,, \tag{2c}$$

with T_{c0} the transition temperature for $\tau=\infty$.

Finally, the free-energy functional corresponding to Eq. (2) is given by[6,33]

$$F_{\rm s} = F_{\rm n} + \int d\mathbf{r}\Bigg\{\frac{(\boldsymbol{\nabla}\times\mathbf{A})^2}{8\pi} + N(0)|\Delta(\mathbf{r})|^2\ln\frac{T}{T_{c0}} + 2\pi TN(0)\sum_{n=0}^{\infty}\left[\frac{|\Delta(\mathbf{r})|^2}{\varepsilon_n} - \langle I(\varepsilon_n,\mathbf{k}_{\rm F},\mathbf{r})\rangle\right]\Bigg\}, \tag{3}$$

where F_n is the free energy in the normal state and I is defined by

$$I \equiv \Delta^* f + \Delta f^\dagger + 2\varepsilon_n(g-1) + \hbar\frac{f\langle f^\dagger\rangle + \langle f\rangle f^\dagger}{4\tau} + \hbar\frac{g\langle g\rangle - 1}{2\tau} - \hbar\frac{f^\dagger\,\mathbf{v}_{\rm F}\cdot\boldsymbol{\partial} f - f\,\mathbf{v}_{\rm F}\cdot\boldsymbol{\partial}^* f^\dagger}{2(g+1)}\,. \tag{4}$$

Indeed, functional differentiations of Eq. (3) with respect to f, Δ, and $\tilde{\mathbf{A}}$ lead to Eqs. (2a), (2b), and (2c), respectively.

B. Operators and basis functions

We first express the gradient operator in Eq. (2a) as

$$\mathbf{v}_{\rm F}\cdot\boldsymbol{\partial} = \frac{\bar{v}_{\rm F+}^*(a+\tilde{A}) - \bar{v}_{\rm F+}(a^\dagger+\tilde{A}^*)}{\sqrt{2}l_{\rm c}}\,. \tag{5}$$

Here a and $a^\dagger$ are the boson operators:

$$\begin{bmatrix} a \\ a^\dagger \end{bmatrix} = \frac{l_{\rm c}}{\sqrt{2}}\begin{bmatrix} c_1 & ic_2 \\ -c_1^* & ic_2^* \end{bmatrix}\begin{bmatrix} \nabla_x \\ \nabla_y - 2\pi iBx/\Phi_0 \end{bmatrix}, \tag{6a}$$

with $l_{\rm c} \equiv \sqrt{\Phi_0/2\pi B}$ and $c_1c_2^* + c_1^*c_2 = 2$, and $\tilde{A}$ and $\bar{v}_{\rm F+}$ are defined by

$$\tilde{A} \equiv -i\frac{\sqrt{2}\pi l_{\rm c}}{\Phi_0}(c_1\tilde{A}_x + ic_2\tilde{A}_y)\,, \tag{6b}$$

$$\bar{v}_{\rm F+} \equiv c_2 v_{{\rm F}x} + ic_1 v_{{\rm F}y}\,, \tag{6c}$$

respectively. The constants (c_1,c_2) can be fixed appropriately to make the subsequent calculations efficient. A convenient choice[25] is to impose the condition that the gradient term in the Ginzburg-Landau equation be expressed in terms of $a^\dagger a$ without using aa and $a^\dagger a^\dagger$, i.e., the pair potential near T_c be described in terms of the lowest Landau level only. Alternatively, one may follow Graser *et al.*[10] to change them at every temperature and magnetic field so as to make the free-energy within the lowest-Landau-level approximation smallest.

Using Eq. (6a), we can make up a set of basis functions to describe arbitrary vortex-lattice structures as[27]

$$\begin{aligned}\psi_{N\mathbf{q}}(\mathbf{r}) = \sqrt{\frac{2\pi l_{\rm c}}{c_1 a_2\sqrt{\pi}\,V}}\sum_{n=-\mathcal{N}_{\rm f}/2+1}^{\mathcal{N}_{\rm f}/2}&\exp\left[iq_y\left(y+\frac{l_{\rm c}^2 q_x}{2}\right)\right]\\ &\times\exp\left[i\frac{na_{1x}}{l_{\rm c}^2}\left(y+l_{\rm c}^2q_x-\frac{na_{1y}}{2}\right)\right]\\ &\times\exp\left[-\frac{c_1c_2}{2}\left(\frac{x-l_{\rm c}^2q_y-na_{1x}}{c_1l_{\rm c}}\right)^2\right]\\ &\times\frac{1}{\sqrt{2^N N!}}H_N\left(\frac{x-l_{\rm c}^2q_y-na_{1x}}{c_1l_{\rm c}}\right)\,.\end{aligned} \tag{7}$$

Here $N = 0,1,2,\cdots$ denotes the Landau level, $\mathbf{q}$ is an arbitrary chosen magnetic Bloch vector characterizing the broken translational symmetry of the vortex lattice and specifying the core locations, and V is the volume of the system. The quantities a_{1x}, a_{1y} and a_2 are the components of the basic vectors $\mathbf{a}_1$ and $\mathbf{a}_2$ in the xy plane, respectively, with $\mathbf{a}_2 \parallel \hat{\mathbf{y}}$ and $a_{1x}a_2 = 2\pi l_{\rm c}^2$, $\mathcal{N}_{\rm f}^2$ denotes the number of the flux quantum in the system, and $H_N(x) \equiv {\rm e}^{x^2}\left(-\frac{d}{dx}\right)^N{\rm e}^{-x^2}$ is the Hermite polynomial. The basis functions are both orthonormal and complete, satisfying $a\psi_{N\mathbf{q}} = \sqrt{N}\psi_{N-1\mathbf{q}}$ and $a^\dagger\psi_{N\mathbf{q}} = \sqrt{N+1}\psi_{N+1\mathbf{q}}$.

C. Algebraic Eilenberger equations

We now expand Δ, f, and $\tilde{A}$ in the basis functions of the vortex lattice as

$$\Delta(\mathbf{r}) = \sqrt{V}\sum_{N=0}^{\infty}\Delta_N\,\psi_{N\mathbf{q}}(\mathbf{r})\,, \tag{8a}$$

$$f(\varepsilon_n,\mathbf{k}_{\rm F},\mathbf{r}) = \sqrt{V}\sum_{N=0}^{\infty} f_N(\varepsilon_n,\mathbf{k}_{\rm F})\,\psi_{N\mathbf{q}}(\mathbf{r})\,, \tag{8b}$$

$$\tilde{A}(\mathbf{r}) = \sum_{\mathbf{K}\neq\mathbf{0}} \tilde{A}_{\mathbf{K}} e^{i\mathbf{K}\cdot\mathbf{r}}\,, \tag{8c}$$

where $\mathbf{K}$ is the reciprocal-lattice vector.[27] Substituting Eq. (8) into Eq. (2) and using the orthogonality of the basis functions, Eq. (2) is transformed into a set of algebraic equations for $\{f_N\}$, $\{\Delta_N\}$, and $\{\tilde{A}_{\mathbf{K}}\}$ as

$$\begin{aligned}&\varepsilon_n f_N + \bar{\beta}^*\sqrt{N+1} f_{N+1} - \bar{\beta}\sqrt{N} f_{N-1}\\ &= \frac{1}{\sqrt{V}}\int \psi^*_{N\mathbf{q}}\left(\Delta\phi g + \hbar\frac{\langle f\rangle g - \langle g\rangle f}{2\tau} - \bar{\beta}^*\tilde{A} + \bar{\beta}\tilde{A}^*\right) d\mathbf{r}\,, \end{aligned}\tag{9a}$$

$$\Delta_N \ln\frac{T_{c0}}{T} = 2\pi T\sum_{n=0}^{\infty}\left[\frac{\Delta_N}{\varepsilon_n} - \langle\phi(\mathbf{k}_{\rm F}) f_N(\varepsilon_n,\mathbf{k}_{\rm F})\rangle\right], \tag{9b}$$

$$\tilde{A}_{\mathbf{K}} = -\frac{16\pi^2 N(0)T}{(Kl_{\rm c}B)^2 V}\sum_{n=0}^{\infty}\int \langle\beta\, g(\varepsilon_n,\mathbf{k}_{\rm F},\mathbf{r})\rangle e^{-i\mathbf{K}\cdot\mathbf{r}} d\mathbf{r}\,, \tag{9c}$$

with

$$\bar{\beta} \equiv \frac{\hbar(c_2 v_{{\rm F}x} + i c_1 v_{{\rm F}y})}{2\sqrt{2} l_{\rm c}}\,, \quad \beta \equiv \frac{\hbar(c_1 v_{{\rm F}x} + i c_2 v_{{\rm F}y})}{2\sqrt{2} l_{\rm c}}\,. \tag{10}$$

Together with the equation to determine H_{c2} derived recently,[25] the above coupled equations form a basis for efficient numerical calculations of the Eilenberger equations for vortex-lattice states with arbitrary Fermi-surface structures.

D. Numerical procedures

For a given vortex-lattice structure specified by the basic vectors $\mathbf{a}_1$ and $\mathbf{a}_2$ in Eq. (7), the coupled equation (9) may be solved iteratively in order of Eqs. (9a), (9b), and (9c) by adopting a standard technique to solve nonlinear equations.[40] A convenient starting point is to put $\Delta_N^{(0)} = \delta_{N0}\Delta(T)\sqrt{1-B/H_{c2}}$, $f_N = 0$, and $\tilde{A}_{\mathbf{K}} = \mathbf{0}$ on the right-hand of Eq. (9a), where $\Delta(T)$ is the angle-averaged energy gap in zero field. In this connection, it may be worth noting that the tridiagonal matrix constructed from the coefficients of f_N on the left-hand side of Eq. (9a) can be inverted analytically.[25] The Fermi-surface integrals $\langle\cdots\rangle$ can be performed as described in Sec. IV of Ref. 25. In contrast, integrations over $\mathbf{r}$ in Eqs. (9a) and (9c) may be carried out as follows: At the beginning of each calculation, we prepare $\psi_{N\mathbf{q}}(\mathbf{r})$ and $e^{i\mathbf{K}\cdot\mathbf{r}}$ at equally spaced $N_{\rm int}\times N_{\rm int}$ discrete points in a unit cell. We then construct $\Delta(\mathbf{r})$, $f(\varepsilon_n,\mathbf{k}_{\rm F},\mathbf{r})$, $\tilde{A}(\mathbf{r})$, and $g=(1-ff^\dagger)^{1/2}$ on those points by Eqs. (8) with restricting the summations to those satisfying $N\le N_{\rm c}$ and $|\mathbf{K}|\le K_{\rm c}$, where $N_{\rm c}$ and $K_{\rm c}$ are some cutoffs. Now, the integrations can be performed by the trapezoidal rule; its convergence is excellent for periodic functions. Also, the summation over n in Eq. (9b) is restricted in the actual calculations to those satisfying $|\varepsilon_n|\le\varepsilon_{\rm c}$. The convergence can be checked by increasing $N_{\rm int}$, $N_{\rm c}$, $K_{\rm c}$, and $\varepsilon_{\rm c}$. Finally, the vortex-lattice structure can be fixed by requiring that the free energy (3) be minimum.

E. Thermodynamic quantities

Once Δ, f, and $\tilde{\mathbf{A}}$ are determined as above, we can calculate thermodynamic quantities of the vortex-lattice state. Specifically, the magnetization M due to supercurrent and the entropy $S_{\rm s}$ are obtained by[34]

$$\begin{aligned}-4\pi M = \frac{1}{BV}\int d\mathbf{r}\Big[&(\nabla\times\tilde{\mathbf{A}})^2\\ &+2\pi^2 N(0)T\sum_{n=0}^{\infty}\left\langle\frac{f^\dagger\mathbf{v}_{\rm F}\cdot\boldsymbol{\partial} f - f\mathbf{v}_{\rm F}\cdot\boldsymbol{\partial}^* f^\dagger}{g+1}\right\rangle,\end{aligned}\tag{11a}$$

$$\begin{aligned}S_{\rm s} = S_{\rm n} - \frac{N(0)}{T}\int d\mathbf{r}\Big\{&|\Delta(\mathbf{r})|^2\\ &-2\pi T\sum_{n=0}^{\infty}\left[\langle I(\varepsilon_n,\mathbf{k}_{\rm F},\mathbf{r})\rangle + 2\varepsilon_n\langle g-1\rangle\right]\Big\},\end{aligned}\tag{11b}$$

respectively, where $S_{\rm n}\equiv 2\pi^2 VN(0)T/3$ is the entropy in the normal state and I is defined by Eq. (4). Also, when it is much smaller than the diamagnetism by supercurrent, the magnetization $M_{\rm sP}$ due to Pauli paramagnetism can be calculated by[34]

$$M_{\rm sP} = M_{\rm nP}\left[1 - \frac{2\pi T}{V}\sum_{n=0}^{\infty}\int d\mathbf{r}\,\frac{\partial\langle g\rangle}{\partial\varepsilon_n}\left(1+\frac{\nabla\times\tilde{\mathbf{A}}}{B}\right)^2\right], \tag{11c}$$

where $M_{\rm nP}\equiv 2VN(0)\mu_{\rm B}^2 B$ with $\mu_{\rm B}$ the Bohr magneton. The quantity

$$\frac{\partial g}{\partial\varepsilon_n} = -\frac{1}{2(1-ff^\dagger)^{1/2}}\left(f\frac{\partial f^\dagger}{\partial\varepsilon_n} + \frac{\partial f}{\partial\varepsilon_n}f^\dagger\right) \tag{12}$$

in Eq. (11c) may be obtained either by numerical differentiations or directly from the equation of differentiating Eq. (2a) with respect to ε_n:

$$\begin{aligned}&\left(\varepsilon_n + \frac{\hbar}{2\tau}\langle g\rangle + \frac{1}{2}\hbar\mathbf{v}_{\rm F}\cdot\boldsymbol{\partial}\right)\frac{\partial f}{\partial\varepsilon_n} + \left(1 + \frac{\hbar}{2\tau}\frac{\partial\langle g\rangle}{\partial\varepsilon_n}\right) f\\ &= \left(\Delta\phi + \frac{\hbar}{2\tau}\langle f\rangle\right)\frac{\partial g}{\partial\varepsilon_n} + \frac{\hbar}{2\tau}\frac{\partial\langle f\rangle}{\partial\varepsilon_n} g\,.\end{aligned}\tag{13}$$

This equation can be solved similarly as Eq. (2a).

III. RESULTS

We now present numerical results for two-dimensional systems with the cylindrical Fermi surface which is placed in the xy plane perpendicular to $\mathbf{H}$. We have considered a couple of energy gaps:

$$\phi(\mathbf{k}_{\rm F}) = \begin{cases} 1 & : s\text{-wave} \\ \sqrt{2}\,(\hat{k}_{{\rm F}x}^2 - \hat{k}_{{\rm F}y}^2) & : d_{x^2-y^2}\text{-wave} \end{cases} . \quad (14)$$

Then it is convenient to set $c_1 = c_2 = 1$ in Eq. (6). There is another parameter in the system corresponding to the Ginzburg-Landau parameter κ. We have fixed it by

$$\kappa_0 \equiv \frac{(\hbar c/2e)\Delta(0)}{\sqrt{4\pi N(0)}\,\hbar^2 v_{\rm F}^2} = \begin{cases} 10 & : s\text{-wave} \\ 7 & : d_{x^2-y^2}\text{-wave} \end{cases} , \quad (15)$$

with $\Delta(0)$ the angle-averaged energy gap at $T = 0$. It follows from Eq. (46) of Ref. 33 that Eq. (15) corresponds to $\kappa = 49$ and 40 for the s- and $d_{x^2-y^2}$-wave pairings in the clean limit, respectively, and $\kappa = 1300$ for the s-wave pairing with $\tau = 0.01\hbar/\Delta(0)$. The vortex-lattice structure has been fixed as hexagonal (square) for the s-wave ($d_{x^2-y^2}$-wave) pairing so that finite contributions in the expansion (8a) come only from $N = 0, 6, 12, \cdots$ ($N = 0, 4, 8, \cdots$) Landau levels.

Equation (9) for the above model has been solved with the procedure of Sec. IID over $0.05H_{c2} \le B \le H_{c2}$. The value $N_{\rm cut}$ is chosen as 30 (16) for the s-wave ($d_{x^2-y^2}$-wave) pairing. On the other hand, we have set $\varepsilon_{\rm c} = 20T_c$ ($50T_c$) at $T = 0.9T_c$ ($0.3T_c$). These values have been enough to get the convergence. Using Δ, f, and $\tilde{A}$ thus obtained, we have calculated the magnetization by supercurrent, the entropy, and the magnetization by Pauli Paramagnetism by Eqs. (11a), (11b), and (11c), respectively.

Figure 1 presents magnetic-field dependence of the magnetization by supercurrent for the s- and $d_{x^2-y^2}$-wave pairings in the clean limit at several temperatures. In both cases, the initial slope at $B = H_{c2}$ gradually decreases as the temperature is lowered, implying a monotonic increase of the Maki parameter[41] $\kappa_2(T)$ as $T \to 0$. This feature of $\kappa_2(T)$ has also been predicted in the case of the three-dimensional spherical Fermi surface with the s-wave pairing.[33,41,42,43] Unlike the three dimensional case,[33,42,43] however, the slope in these two-dimensional cases remains finite and does not approach 0 even in the clean limit of $T \to 0$, in agreement with a previous calculation of κ_2.[33] The curves at low temperatures become more and more concave upward, thereby compensating the initial reduction of the magnetization. The temperature variation is slightly larger for the $d_{x^2-y^2}$-wave pairing than the s-wave pairing.

Figure 2 shows the expansion coefficients Δ_N in Eq. (8a) as a function of B/H_{c2} for the s- and $d_{x^2-y^2}$-wave pairings in the clean limit at $T = 0.3T_c$. Compared with the case near T_c,[27] the mixing of higher Landau levels develops from higher fields. However, the

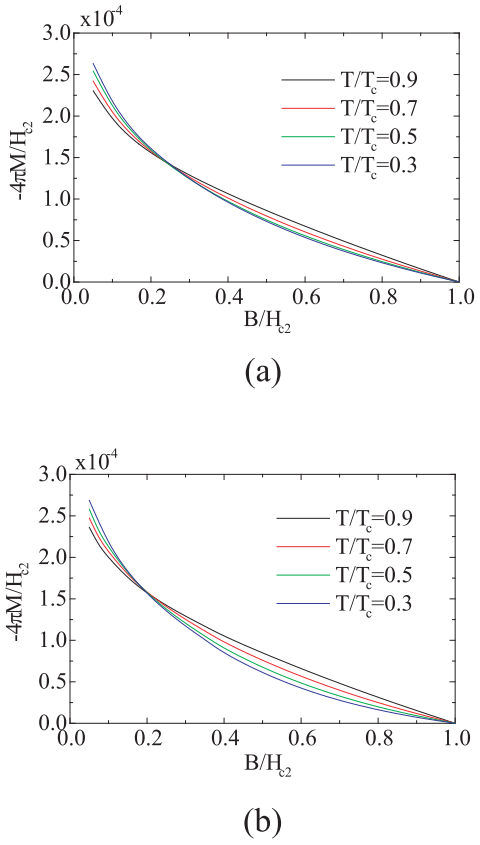

FIG. 1: The magnetization by supercurrent as a function of B/H_{c2} in the clean limit. (a) s-wave; (b) $d_{x^2-y^2}$-wave. The temperatures are $T/T_{\rm c} = 0.9$, 0.7, 0.5, and 0.3 from top to bottom in the high-field region.

contribution is still $\sim 0.1\Delta_0$ even around $B = 0.1H_{c2}$. This fact implies that the Pesch approximation[7] is excellent down to $H \sim 0.1H_{c2}$ for the two-dimensional cases with the isotropic Fermi surface. This may not be the case for systems with complicated Fermi surfaces, however, as suggested by the fact that there is already an amount of higher-Landau-level contributions at H_{c2} in those cases.[24,25,26] The Pesch approximation may be improved to some degree by the procedure of Graser *et al.*[10] to change c_1 and c_2 in Eq. (6a) at every temperature and magnetic field so that the free-energy is smallest.

Figures 3 and 4 plot the entropy $S_{\rm s}$ and the magnetization $M_{\rm sP}$ due to Pauli paramagnetism, respectively, as a function of B/H_{c2} for the s- and $d_{x^2-y^2}$-wave pairings in the clean limit at several temperatures. To see

TABLE I: The exponent $\alpha_{\rm S}$ of Eq. (16a) for the s- and $d_{x^2-y^2}$-wave pairings in the clean limit calculated by the best fit to the numerical data of Fig. 3.

$T/T_{\rm c}$	0.9	0.7	0.5	0.3
α_S (s-wave)	0.73	0.69	0.66	0.63
α_S (d-wave)	0.72	0.66	0.59	0.52

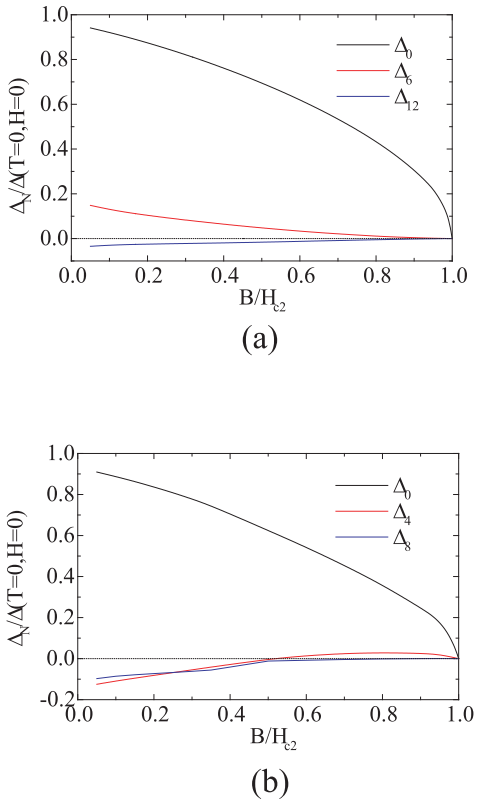

FIG. 2: The expansion coefficients Δ_N in Eq. (8a) as a function of B/H_{c2} in the clean limit at $T = 0.3T_c$: (a) s-wave pairing where the curves are Δ_0, Δ_6, and Δ_{12} from top to bottom; (b) $d_{x^2-y^2}$-wave pairing where the curves are Δ_0, Δ_4, and Δ_8 from top to bottom near H_{c2}.

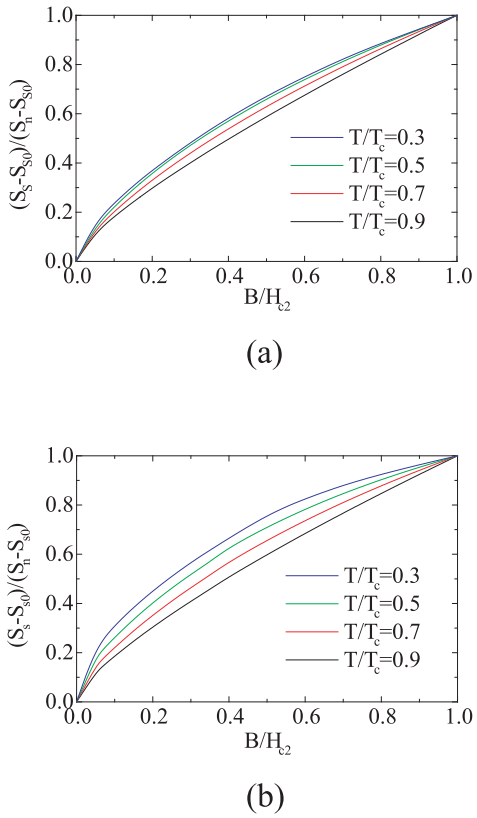

FIG. 3: The entropy S_s as a function of B/H_{c2}. (a) s-wave; (b) $d_{x^2-y^2}$-wave. The temperatures are $T/T_c = 0.9$, 0.7, 0.5, and 0.3 from bottom to top. They are normalized to vary from 1 at $B = H_{c2}$ to 0 at $B = 0$.

the field dependence clearly, the entropy is normalized by using $S_{s0} \equiv S_s(B = 0)$ and $S_n \equiv S_s(B = H_{c2})$ as $(S_s - S_{s0})/(S_n - S_{s0})$; it varies from 1 to 0 for $H_{c2} \geq B \geq 0$. The same normalization is adopted for M_{sP}. All curves deviate upwards from the linear behavior $\propto B/H_{c2}$ and become more and more convex upward as $T \to 0$. This tendency is more conspicuous for the $d_{x^2-y^2}$-wave pairing due to the residual low-energy density of states. To see the behavior quantitatively, we have fitted our numerical data by the formulas:

$$\frac{S_s - S_{s0}}{S_n - S_{s0}} = \left(\frac{B}{H_{c2}}\right)^{\alpha_S}, \qquad (16a)$$

TABLE II: The exponent α_χ of Eq. (16b) for the s- and $d_{x^2-y^2}$-wave pairings in the clean limit calculated by the best fit to the numerical data of Fig. 4.

T/T_c	0.9	0.7	0.5	0.3
α_χ (s-wave)	0.71	0.67	0.63	0.63
α_χ (d-wave)	0.70	0.63	0.56	0.49

$$\frac{M_{sP} - M_{sP0}}{M_n - M_{sP0}} = \left(\frac{B}{H_{c2}}\right)^{\alpha_\chi}. \qquad (16b)$$

To confirm the numerical results, we first estimated α_S and α_χ for the s-wave pairing by using only the data of $0.85H_{c2} \leq B \leq 0.95H_{c2}$. Although not presented here, the procedure excellently reproduced the values of a previous calculation near H_{c2},[34] as they should.

Table I shows the exponent α_S obtained by the best fit to the data of $0.05H_{c2} \leq B \leq 0.95H_{c2}$ in Fig. 3. The value of the $d_{x^2-y^2}$ pairing at $T/T_c = 0.9$ is almost the same as the corresponding s-wave result. As the temperature is decreased, however, the $d_{x^2-y^2}$-wave exponent decreases more rapidly so that the curve in Fig. 3(b) becomes more convex upward; this is due to the residual low-energy density of states of the $d_{x^2-y^2}$-wave pairing. Table II presents another exponent α_χ obtained by the best fit to the data of $0.05H_{c2} \leq B \leq 0.95H_{c2}$ in Fig. 4. Each value is fairly close to the corresponding one for α_S, as may be expected from the fact that both quantities probe the zero-energy density of states. In this context, Ichioka *et al.*[17] calculated the field dependence

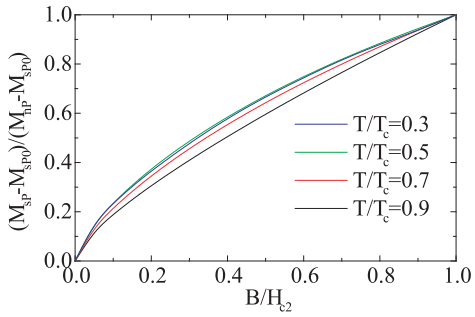

(a)

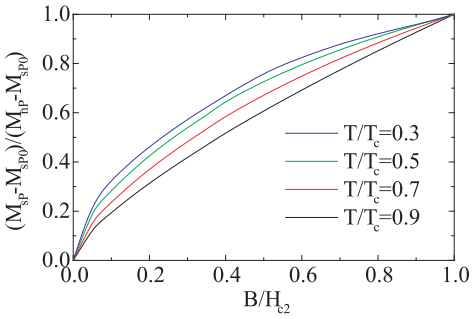

(b)

FIG. 4: The magnetization $M_{\rm sP}$ by Pauli paramagnetism as a function of B/H_{c2}. (a) s-wave; (b) $d_{x^2-y^2}$-wave. The temperatures are $T/T_{\rm c}$ = 0.9, 0.7, 0.5 and 0.3 from bottom to top. They are normalized to vary from 1 at $B=H_{c2}$ to 0 at $B=0$.

of the zero-energy density of states $N(0)$ at $T/T_c=0.5$ to find $N(0)\propto(B/H_{c2})^{0.67}$ and $N(0)\propto(B/H_{c2})^{0.41}$ for the s- and $d_{x^2-y^2}$-wave pairings, respectively. Our estimates for $\alpha_S(T\to0)$ and $\alpha_\chi(T\to0)$ are somewhat smaller (larger) for the s-wave ($d_{x^2-y^2}$-wave) pairing.

Experiments on the T-linear specific-heat coefficient $\gamma_{\rm s}(B)$ have been performed for clean V_3Si,[44] $NbSe_2$,[45,46,47,48] and $CeRu_2$.[49] The quantity $\gamma_{\rm s}(B)/\gamma_n$ coincides for $T\to0$ with $(S_s-S_{s0})/(S_n-S_{s0})$ of Fig. 3. Those data all show marked upward deviations from the linear behavior γ_nB/H_{c2}, indicating that it is a common feature among clean superconductors irrespective of the energy-gap symmetry. Sonier *et al.*[47] thereby extracted the exponent 0.66 for the field dependence of $\gamma_{\rm s}(B)$ as $T\to0$, in good agreement with the result 0.67 by Ichioka *et al.*[17] for the clean two-dimensional s-wave model. However, a more recent experiment by Hanaguri *et al.*[48] reported a different exponent 0.5. It should also be noted that $NbSe_2$ has three kinds of Fermi surfaces and one of them is quite different in structure from the cylinder. There also exists a recent experiment which indicates existence of different superconducting energy

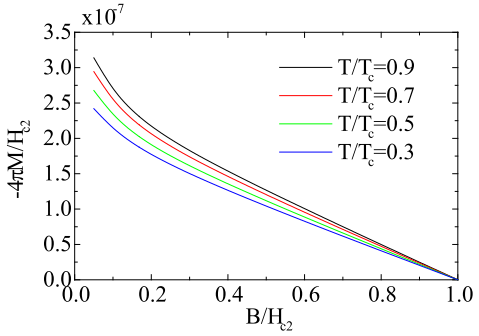

FIG. 5: Magnetization by supercurrent as a function of B/H_{c2} for the s-wave pairing with $\tau=\hbar/\Delta(0)$. The temperatures are $T/T_{\rm c}=0.9$, 0.7, 0.5, and 0.3 from top to bottom.

gaps on different Fermi surfaces.[3] Hence the agreement between the experiment by Sonier *et al.*[47] and the theory by Ichioka *et al.*[17] might be an artifact and should be confirmed by more detailed experiments as well as theories incorporating both Fermi-surface and gap structures. In this context, it is worth noting that no detailed experiments have been performed on the field dependence of $\gamma_{\rm s}(B)$ even for the classic type-II superconductors V and Nb, although early experiments[50,51] suggest similar upward deviations from the linear behavior γ_nB/H_{c2}.

We next focus on the s-wave pairing in the dirty limit. Figure 5 shows the magnetization for $\tau=0.01\hbar/\Delta(0)$ as a function of B/H_{c2}. Compared with the clean-limit results of Fig. 1(a), we observe an extended linearity down to $B/H_{c2}\sim0.2$ irrespective of the temperature. The decrease of the initial slope for $T\to0$ is as expected from the temperature dependence of the Maki parameter κ_2.[41] By scaling this change of the initial slope, all the curves almost fall onto a single curve. This is a marked feature in the dirty limit which is absent in the clean-limit result of Fig. 1(a).

Figure 6 shows the field dependences of $S_{\rm s}$ and $M_{\rm sP}$ for $\tau=0.01\hbar/\Delta(0)$ at various temperatures. Table III presents the corresponding exponents $\alpha_{\rm s}$ and α_χ obtained from the data of $0.5H_{c2}\le B\le0.95H_{c2}$; unlike the clean-limit case, it has been impossible to fit the whole region by a single exponent, especially at intermediate temperatures, as may be realized from Fig. 6. Compared with Figs. 3(a) and 4(a), the curves are more monotonic with the almost linear behavior $\propto B/H_{c2}$. Looking at the temperature dependence more closely, however, we observe a change from a convex-upward behavior at high tem-

TABLE III: The exponents $\alpha_{\rm S}$ and α_χ for the s-wave pairing with $\tau=0.01\hbar/\Delta(0)$ calculated by the best fit to the numerical data of $0.5H_{c2}\le B\le0.95H_{c2}$.

$T/T_{\rm c}$	0.9	0.7	0.5	0.3
α_S	0.84	0.88	0.92	1.10
α_χ	0.84	0.89	0.99	1.15

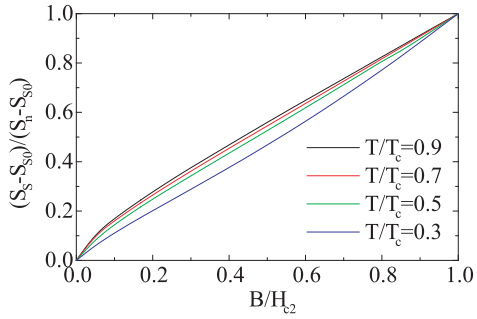

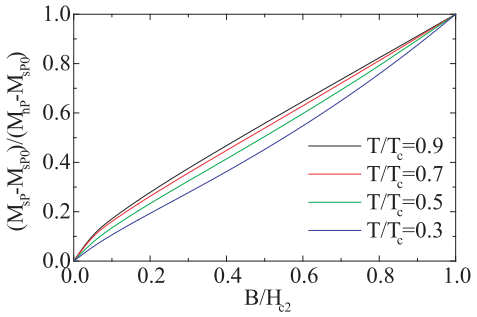

FIG. 6: (a) The entropy $S_{\rm S}$ and (b) the magnetization $M_{\rm sP}$ by Pauli paramagnetism as a function of B/H_{c2} for the s-wave pairing with $\tau = 0.01\hbar/\Delta(0)$. The temperatures are $T/T_{\rm c} = 0.9$, 0.7, 0.5 and 0.3 from top to bottom.

peratures to a convex-downward behavior at low temperatures, in agreement with a previous calculation near H_{c2}.[34] This feature also appears in the field dependence of the zero-energy density of states as calculated recently by Miranović *et al.*[22] The convex-downward behavior at $T = 0.3T_c$ may become more pronounced at lower temperatures to be observable experimentally.

IV. SUMMARY

We have developed an alternative method to solve the Eilenberger equations for the vortex-lattice state. The main analytic formulas are given in Sec. IIC together with the numerical procedure to solve them in Sec. IID. This method, which directly extends the H_{c2} equation[25,26] to lower fields, has a potential applicability to systems with complicated Fermi surfaces and/or gap structures to carry out detailed calculations on the field dependences of thermodynamic quantities for various type-II superconductors.

Using it, we have calculated the field dependences of the magnetization by supercurrent, the mixing of higher Landau levels in the pair potential, the entropy, and the Pauli paramagnetism for the two-dimensional s- and $d_{x^2-y^2}$-wave pairings in the clean and dirty limits at various temperatures. Previous results near H_{c2} for the s-wave pairing[33,34] have been reproduced adequately and extended to lower fields to clarify the overall field dependences. The differences between the s- and $d_{x^2-y^2}$-wave pairings are quite small at high temperatures but develop gradually as the temperature is lowered, reflecting the marked difference in the low-energy density of states between the two cases. The field dependences of the entropy and Pauli paramagnetism in the clean limit at low temperatures present convex-upward behaviors for both pairings. In contrast, the curves of the s-wave pairing in the dirty limit are more monotonic and fairly close to the linear behavior, but also acquire downward curvature at low temperatures. As for the magnetization by supercurrent, there is a wide region of linear field dependence from H_{c2} both at high temperatures and in the dirty limit. The region shrinks in the clean limit as the temperature is lowered, and the curve acquires pronounced upward curvature. It is also found that the mixing of higher Landau levels in the pair potential is small for $B \gtrsim 0.1H_{c2}$ but develops rapidly as the field is further decreased.

Acknowledgments

This work is supported by a Grant-in-Aid for Scientific Research from the Ministry of Education, Culture, Sports, Science, and Technology of Japan, and also from the 21st century COE program "Topological Science and Technology," Hokkaido University.

[1] A. V. Sologubenko, J. Jun, S. M. Kazakov, J. Karpinski, and H. R. Ott, Phys. Rev. B **66**, 014504 (2001).
[2] K. Izawa, Y. Nakajima, J. Goryo, Y. Matsuda, S. Osaki, H. Sugawara, H. Sato, P. Thalmeier, and K. Maki, Phys. Rev. Lett. **90**, 117001 (2003).
[3] E. Boaknin, M. A. Tanatar, J. Paglione, D. Hawthorn, F. Ronning, R. W. Hill, M. Sutherland, L. Taillefer, J. Sonier, S. M. Hayden, and J. W. Brill, Phys. Rev. Lett. **90**, 117003 (2003).
[4] H. Aoki, T. Sakakibara, H. Shishido, R. Settai, Y. Onuki, P. Miranović, and K. Machida, J. Phys. Condens. Matter **16**, L13 (2004).
[5] K. Deguchi, Z. Q. Mao, H. Yaguchi, and Y. Maeno, Phys. Rev. Lett. **92**, 047002 (2004).
[6] G. Eilenberger: Z. Phys. **214**, 195 (1968).
[7] W. Pesch, Z. Phys. B **21**, 263 (1975).

[8] I. Vekhter and A. Houghton, Phys. Rev. Lett. **83**, 4626 (1999).
[9] T. Dahm, S. Graser, C. Iniotakis, and N. Schopohl, Phys. Rev. B **66**, 144515 (2002).
[10] S. Graser, T. Dahm, and N. Schopohl, Phys. Rev. B **69**, 014511 (2004).
[11] M. Udagawa, Y. Yanase, and M. Ogata, cond-mat/0408643.
[12] H. Kusunose, Phys. Rev. B **70**, 054509 (2004).
[13] U. Klein, J. Low Temp. Phys. **69**, 1 (1987).
[14] U. Klein, Phys. Rev. B **40**, 6601 (1989).
[15] M. Ichioka, N. Hayashi, N. Enomoto, and K. Machida, Phys. Rev. B **53**, 15316 (1996).
[16] M. Ichioka, N. Hayashi, and K. Machida Phys. Rev. B **55**, 6565 (1997).
[17] M. Ichioka, A. Hasegawa, and K. Machida, Phys. Rev. B **59**, 184 (1999).
[18] M. Ichioka, A. Hasegawa, and K. Machida, Phys. Rev. B **59**, 8902 (1999).
[19] M. Ichioka and K. Machida, Phys. Rev. B **65**, 224517 (2002).
[20] P. Miranović, N. Nakai, M. Ichioka, and K. Machida, Phys. Rev. B **68**, 052501 (2003).
[21] N. Nakai, P. Miranović, M. Ichioka, and K. Machida Phys. Rev. B **70**, 100503 (2004).
[22] P. Miranović, M. Ichioka, and K. Machida Phys. Rev. B **70**, 104510 (2004).
[23] M. Ichioka, K. Machida, N. Nakai, and P. Miranović, Phys. Rev. B **70**, 144508 (2004)
[24] C. T. Rieck and K. Scharnberg, Physica B **163**, 670 (1990).
[25] T. Kita and M. Arai, Phys. Rev. B **70**, 224522 (2004).
[26] M. Arai and T. Kita, J. Phys. Soc. Jpn. **73**, 2924 (2004).
[27] T. Kita, J. Phys. Soc. Jpn. **67**, 2067 (1998).
[28] M. R. Norman, A. H. MacDonald, and H. Akera, Phys. Rev. B**51**, 5927 (1995).
[29] T. Kita, J. Phys. Soc. Jpn. **67**, 2075 (1998).
[30] K. Yasui and T. Kita, Phys. Rev. Lett. **86**, 1836 (1999).
[31] K. Yasui and T. Kita: Phys. Rev. B**66**, 184516 (2002).
[32] T. Kita, J. Phys. Soc. Jpn **73**, 21 (2004).
[33] T. Kita, Phys. Rev. B **68**, 184503 (2003).
[34] T. Kita, Phys. Rev. B **69**, 144507 (2004).
[35] G. Lasher, Phys. Rev. **140**, A523 (1965).
[36] P. M. Marcus, in *Proceeding of the Tenth International Conference on Low Temperarure Physics*, edited by M. P. Malkov *et al.* (Viniti Moscow, 1967), Vol. IIA, p. 345.
[37] E. H. Brandt, Phys. Status Solidi B **51**, 345 (1972).
[38] M. M. Doria, J. E. Gubernatis, and D. Rainer, Phys. Rev. B **41**, 6335 (1990).
[39] We will consider positively charged particles following the convention; the case of electrons can be obtained directly by $\mathbf{A} \rightarrow -\mathbf{A}$, i.e., reversing the magnetic-field direction.
[40] W. H. Press, S. A. Teukolsky, W. T. Vetterling and B. P. Flannery, *Numerical Recipes in C* (Cambridge University Press, Cambridge, 1988) Chap. 9.
[41] K. Maki, Physics **1**, 21 (1964).
[42] K. Maki and T. Tsuzuki, Phys. Rev. **139**, A868 (1965).
[43] G. Eilenberger, Phys. Rev. **153**, 584 (1967).
[44] A.P.Ramirez, Phys. Lett. A 211, 59 (1996).
[45] D. Sanchez, A. Junod, J. Muller, H. Berger, and F. Levy, Physica B **204**, 167 (1995).
[46] M. Nohara, M. Isshiki, F. Sakai, and H. Takagi, J. Phys. Soc. Jpn. **68**, 1078 (1999).
[47] J.E. Sonier, M.F. Hundley, J.D. Thompson, and J.W.Brill, Phys. Rev. Lett. **82**, 4914 (1999).
[48] T. Hanaguri, A. Koizumi, K. Takaki, M. Nohara, H. Takagi, and K. Kitazawa, Physica B **329-333**, 1355 (2003).
[49] M. Hedo, Y. Inada, E. Yamamoto, Y. Haga, Y. Ōnuki, Y. Aoki, T.D. Matsuda, and H. Sato, J. Phys. Soc. Jpn. **67**, 272 (1998).
[50] R. Radebaugh and P.H. Keesom, Phys. Rev. **149**, 217 (1966).
[51] J. Ferreira da Silva, E.A. Burgemeister, and Z. Dokoupil, Physica **41**, 409 (1969).